

## Supplementary figures

### Supplementary Figure 1. Sequence alignment of PLAT from PC1 paralogues

The PKD1 PLAT sequence was aligned to PLAT sequences derived from PKD1L1, PKD1L2, PKD1L3 and PKD1REJ. Fully conserved residues are labeled with a black background. Similar residues are on a grey background. There are 22 fully conserved residues (18.2% of total 116 residues) shown as capital letters in the consensus sequence and 67 similarly conserved residues (55.4% of total 116 residues) represented as lower case letters in the consensus sequence. Eight  $\beta$ -strands are indicated. The calcium binding site (DGD) is colored in red with key residues marked by red dots and is not conserved. The phosphorylation site (RNS) is labeled in green and the key residues indicated by the green colons were conserved in PKD1L1 and PKDREJ. PI4P binding residues are marked in blue and PS binding residues in orange. The residue D3166 bound to both PI4P and PS and is indicated in lower case. Accession numbers: PKD1 (P98161), PKD1L1 (Q8TDX9), PKD1L2 (Q7Z442), PKD1L3 (Q7Z443), PKDREJ (Q9NTG1).

### Supplementary Figure 2. Liposome co-sedimentation and protein lipid bead pull-down assays of MBP-PLAT

A: Representative blot showing that the presence or absence of  $\text{Ca}^{2+}$  ions affects the amount of MBP-PLAT pulled down by PS-liposomes but not PI4P liposomes. Analysis of the gels showed that ~ 74% of wild type MBP-PLAT co-sedimented with PS-liposomes in the presence of  $\text{Ca}^{2+}$  (2 mM) but less than 10% when free  $\text{Ca}^{2+}$  was removed by EGTA (2 mM). MBP protein did not co-sediment with any liposomes tested. Nearly 80% of wild type protein was co-sedimented with PI4P with no significant difference with and without  $\text{Ca}^{2+}$ . Bands highlighted by the red boxes indicate co-sedimented MBP-PLAT.

Lane 1 = total protein added; Lane 2 = protein only supernatant; Lane 3 = protein only pellet;  
Lane 4 = protein + liposome +  $\text{Ca}^{2+}$  supernatant; Lane 5 = protein + liposome +  $\text{Ca}^{2+}$  pellet;  
Lane 6 = protein + liposome -  $\text{Ca}^{2+}$  supernatant; Lane 7 = protein + liposome -  $\text{Ca}^{2+}$  pellet; Lane  
8 = Liposome only supernatant; Lane 9 = Liposome only pellet.

B, C. MBP pull-down experiments with PS-beads (B) and PI4P-beads (C). Similar to the liposome sedimentation assays, MBP-PLAT binding to PS-beads was highly  $\text{Ca}^{2+}$ -dependent whereas binding to PI4P-beads was  $\text{Ca}^{2+}$ -independent. PKA pre-treatment of MBP-PLAT reduced PI4P-binding by 50% but had no effect on PS-binding. Molecular weight of MBP is 43kDa; MBP-PLAT is 57kDa.

Supplementary Figure 3. Peptide and phosphopeptide sequences identified by LC-MS/MS from PLAT pull-down experiments

A. Coomassie gel showing immunoprecipitation of control GFP and YFP-PLAT (arrowheads). Gel lanes were cut into equal slices and binding partners identified by LC-MS/MS.

B. Table showing peptide and phosphopeptide sequences of PLAT or AP2 components identified by LC-MS/MS from pull-down experiments.

Supplementary Figure 4. Structural models of PLAT

A: Initial homology-based model of PC1-PLAT. Residues in green are consistent with experimental NMR data; those in red are inconsistent; and the experimental data provide no structural information on those in magenta. Residues in orange are mobile and have no strongly preferred structure.

B: NMR-refined model of PC1-PLAT. Colour scheme is the same as in (A).

Supplementary Figure 5. Confocal microscopy of stably transfected MDCK II clones expressing YFP-PLAT

A. Three MDCKII clones (clones 1-3) with varying but stable expression of YFP-PLAT all showing localisation at the basolateral membrane. Clone 2 was grown to post-confluence on semi-permeable filters to form a polarised monolayer and to permit cilia formation. Confocal microscopy was then performed with a number of membrane markers and optical sections (x-y and x-z) displayed. The arrows indicate the optical z section displayed for each marker: B.

E-cadherin; C. Desmoplakin; D. ZO-1; E. Acetylated tubulin; F. gp135. YFP-PLAT colocalised with basolateral markers (E-cadherin, desmoplakin and ZO-1) but not with the apical marker, gp135, or to primary cilia (acetylated tubulin). In a minority of cells (1%), YFP-PLAT also colocalised to the basal body (E) but not to the cilia shaft. G. cAMP-dependent internalisation of wild-type, R3164A and R3162C YFP-PLAT in MDCK cells.

#### Supplementary Figure 6. PC2 is required for PC1 surface localisation

A. Co-localisation of double epitope-tagged (Flag-PC1-HA) wild-type PC1 and mutants co-expressed with PC2-Pk in HEK-293 cells. Scale bar = 10 $\mu$ m.

B. Western blotting of HEK293 cells co-transfected with wild-type Flag-PC1-HA or mutants and PC2-Pk. All expressed PC1 proteins showed equivalent full-length (FL), C-terminal Fragment (CTF) and N-terminal Fragment (NTF) as detected with HA and Flag antibodies. Equal expression of PC2-Pk is shown using a Pk antibody.

C, D. Live cell surface labelling of HEK-293 cells expressing wild-type Flag-PC1-HA or a S3164D mutant co-expressed with either PC2-Pk or pcDNA3. The mouse PC1 cDNA contains 3xFlag N-terminal and 3xHA C-terminal epitope tags. PC2 is absolutely required for cell surface labelling of PC1. HA staining was performed following cell permeabilisation to show the total number of cells expressing PC1. Cell surface labelling of PC1 (Anti-Flag) was almost completely absent in the S3164D mutant compared to wild-type PC1 despite equal expression (anti-HA) in the presence of PC2. \*\*\*\*p<0.0001. Scale bar = 10 $\mu$ m.

#### Supplementary Figure 7. Rapamycin-induced targeting of PJ and PJ mutants to the PM in HEK293 and CHO cells

A. A chemical dimerization strategy based on the rapamycin-inducible dimerization of FKBP (FK506 binding protein 12) and FRB (fragment of mTOR that binds rapamycin) domains to recruit inositol phosphatase enzymes acutely to the PM<sup>20</sup>. Constructs encoding an enzymatic chimera of inositol polyphosphate 5-phosphatase E (INPP5E) which converts PI(4,5)P<sub>2</sub> to PI4P and the *S. cerevisiae* Sac1 phosphatase which dephosphorylates PI4P, were used to deplete PM PI4P and PI(4,5)P<sub>2</sub> singly or in combination.

B. Time dependent translocation of RFP-FKBP-PJ to the PM in HEK293 cells induced by addition of 1  $\mu$ M rapamycin after 10 s. Images (grey scale) were captured every 10 s. Scale bar = 10 $\mu$ m.

C. Lyn11-FRB-CFP (cyan) in all four panels showing constitutive PM localisation. Panels showing rapamycin-dependent translocation of PJ, PJ-Sac (with inactivated INPP5E domain), INPP5E (lacking the Sac domain) and PJ-Dead (with inactivated INPP5E and Sac domains) FKBP-RFP fusions (red) to the PM at 90 s (arrows show surface localisation of RFP tagged PJ fusion proteins after addition of rapamycin). Scale bar = 10 $\mu$ m.

D, E. Surface expression of YFP-PLAT following rapamycin induced translocation of PJ or the PJ-Dead mutant to the PM in HEK293 and CHO cells (white arrows show surface localisation of YFP-PLAT after rapamycin; yellow arrows show internalisation of YFP-PLAT following rapamycin-induced translocation of PJ fusion protein). Only translocation of PJ had a significant effect on PM localisation of YFP-PLAT at 15 and 60 m after rapamycin in both cell lines. \*  $p < 0.05$ ; \*\*\* $p < 0.001$  v control. Scale bar = 10 $\mu$ m.

#### Supplementary Figure 8. cAMP mediated endocytosis of YFP-PLAT is dependent on AP2 and ARRB1/2

A-C. YFP-PLAT was co-transfected with scrambled or ARRB1/2 specific siRNA into HEK293 cells. (A) Endocytosis was stimulated by the addition of dbcAMP in scrambled control siRNA transfected cells but this was inhibited in cells transfected with ARRB1 siRNA. Arrows indicate surface expression of YFP-PLAT. Scale bar = 10 $\mu$ m. (B) Knockdown of ARRB1/2 was significantly increased by combining two specific siRNA oligos (ARRB1 siRNA 1+2) confirmed by Western blotting. (C) There was a significant reduction in cAMP mediated endocytosis of YFP-PLAT following ARRB1/2 siRNA knockdown compared to control siRNA. \*\*\* $p < 0.001$  compared to ARRB1/2 siRNA.

D-F. Similar experiments were conducted for YFP-PLAT following siRNA knockdown of AP2M1 in HEK293 cells. (D) Endocytosis was stimulated by the addition of dbcAMP in control siRNA transfected cells but this was inhibited in cells transfected with AP2M1 siRNA. Arrows indicate surface expression of YFP-PLAT. Scale bar = 10 $\mu$ m. (E) Knockdown of AP2M1 was detected by

Western blotting. A non-specific lower MW band is marked (\*). (F) A significant reduction in cAMP mediated endocytosis of YFP-PLAT was detected following AP2M1 siRNA knockdown compared with control siRNA. \*\*\* $p < 0.001$  compared to AP2M1 siRNA.

G. YFP-PLAT and a putative AP2 binding mutant (Y3120N, L3123A) were transiently expressed in HEK293 cells. Arrows indicate surface expression of wild-type or mutant YFP-PLAT. Scale bar = 10 $\mu$ m. Mutant YFP-PLAT showed a significant reduction in cAMP or forskolin mediated internalisation compared to wild type PLAT. \*\*\* $p < 0.001$  YFP-PLAT compared to YFP-PLAT AP2 mutant.

Supplementary Figure 9. Knockdown of endogenous AP2M1 or ARRB1/2 and deglycosylation analysis of endogenous PC1 in the human kidney line, UCL93/3

A, B. Cell surface biotinylation of endogenous PC1 in normal human kidney epithelial cells (UCL93/3). There was a significant reduction in surface labelled PC1 (arrowheads) in cells treated with cAMP compared to controls. In both cAMP and control cells, siRNA knockdown of AP2M1 or ARRB1/2 resulted in an increase in surface labelled PC1 compared to scrambled siRNA controls (Fig. S10a). Blotting with the N-terminal PC1 mAb 7e12 showed the presence of three previously described glycoforms of PC1 in these cells. The bars show the mean ratio of biotinylated PC1 to total PC1 (7e12 blot) from 3 independent experiments.

C. Only the uppermost expressed glycoform of PC1 (NTR), shown to be EndoH-resistant was consistently biotinylated. The two EndoH-sensitive glycoforms (NTS1, NTS2) could represent less mature forms of PC1 which have not yet undergone Golgi maturation.

Supplementary Figure 10. Co-transfection of ARRB1/2 cDNA rescues the effect of siRNA depletion of endogenous ARRB1/2 on PC1-S3164D surface expression

A-C. Co-transfection of rat ARRB1/2 cDNA 'rescues' the increased surface expression seen on depletion of endogenous ARRB1/2 in HEK293 cells. The bars represent the means of three independent experiments. \* $p < 0.05$  vs ARRB1/2 siRNA alone. Lysates of cells transfected with ARRB1/2 siRNA with or without rat ARRB1/2 cDNA blotted with an ARRB1/2 antibody.

D. Quantification of surface biotinylated Na-K-ATPase from the same experiments expressed relative to controls showing a similar pattern of increased surface expression after knockdown of ARRB1/2 and rescue by co-transfected rat ARRB1/2. \* $p < 0.05$ ; \*\* $p < 0.01$ .

#### Supplementary Figure 11. Dynamin mutant inhibits endocytosis of S3164D-PC1

A. HEK293 cells expressing CFP-labelled dynamin or a dominant-negative dynamin K44A mutant were incubated with 25  $\mu\text{g/ml}$  transferrin-594 for 30 m at 37°C. Expression of the dynamin K44A mutant significantly inhibited uptake of labelled transferrin.

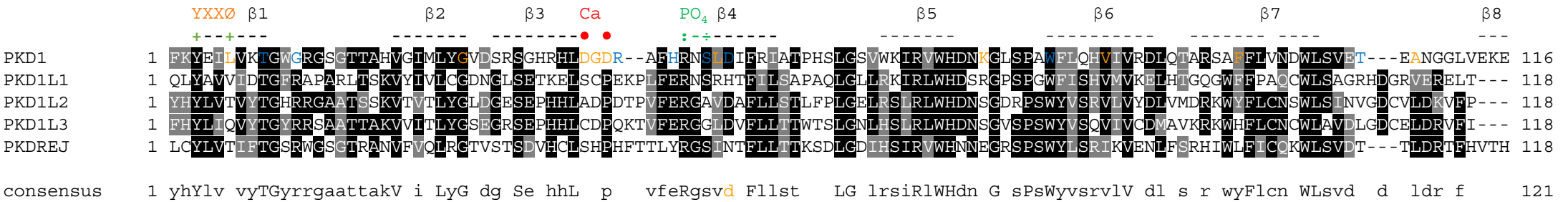
B-E. Cell surface labelling of PC1-S3164D was significantly increased by co-expression of the dynamin mutant (K44A). Co-transfected cells were visualised by CFP fluorescence. \* $p < 0.05$ ; \*\*\* $p < 0.001$  v pcDNA3. Scale bar = 10 $\mu\text{m}$ .

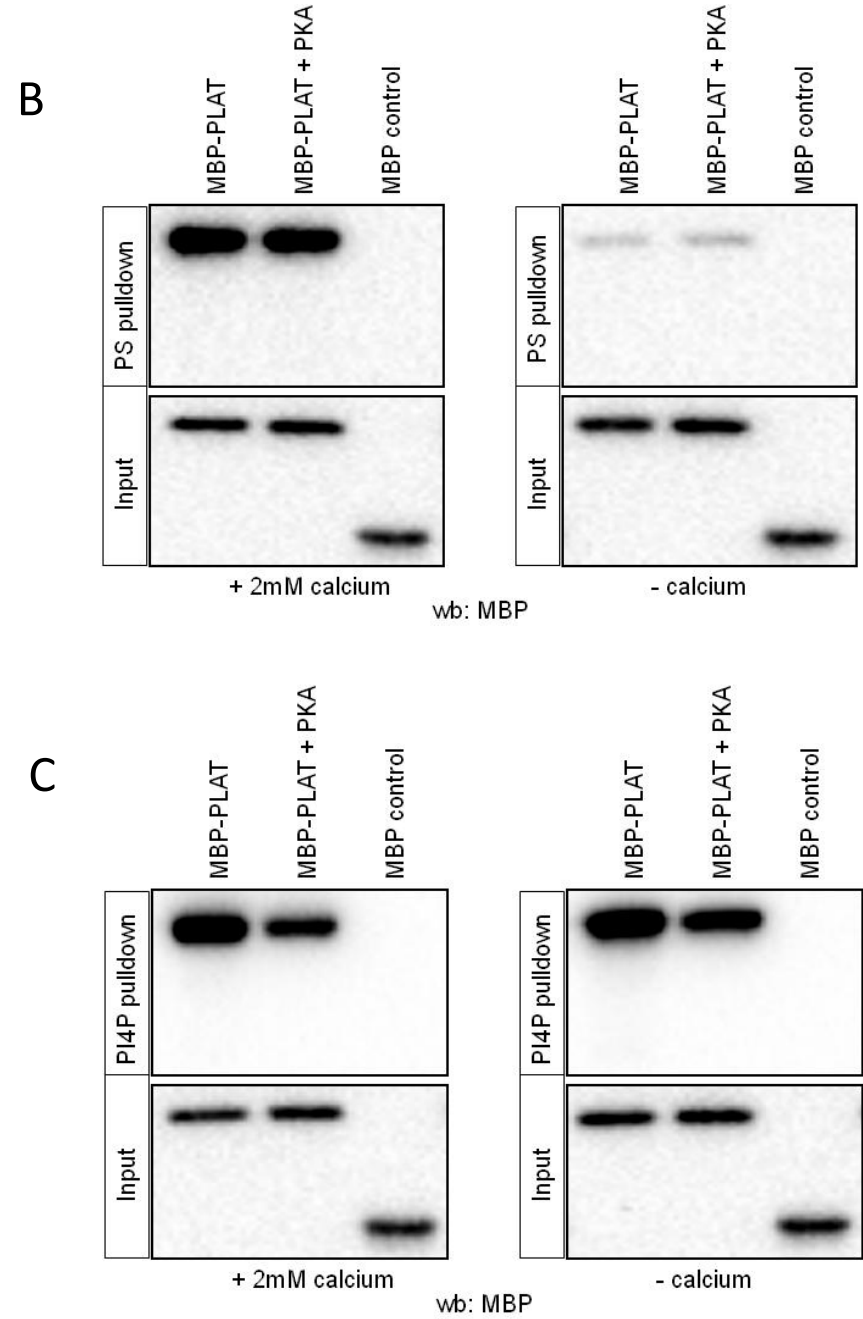
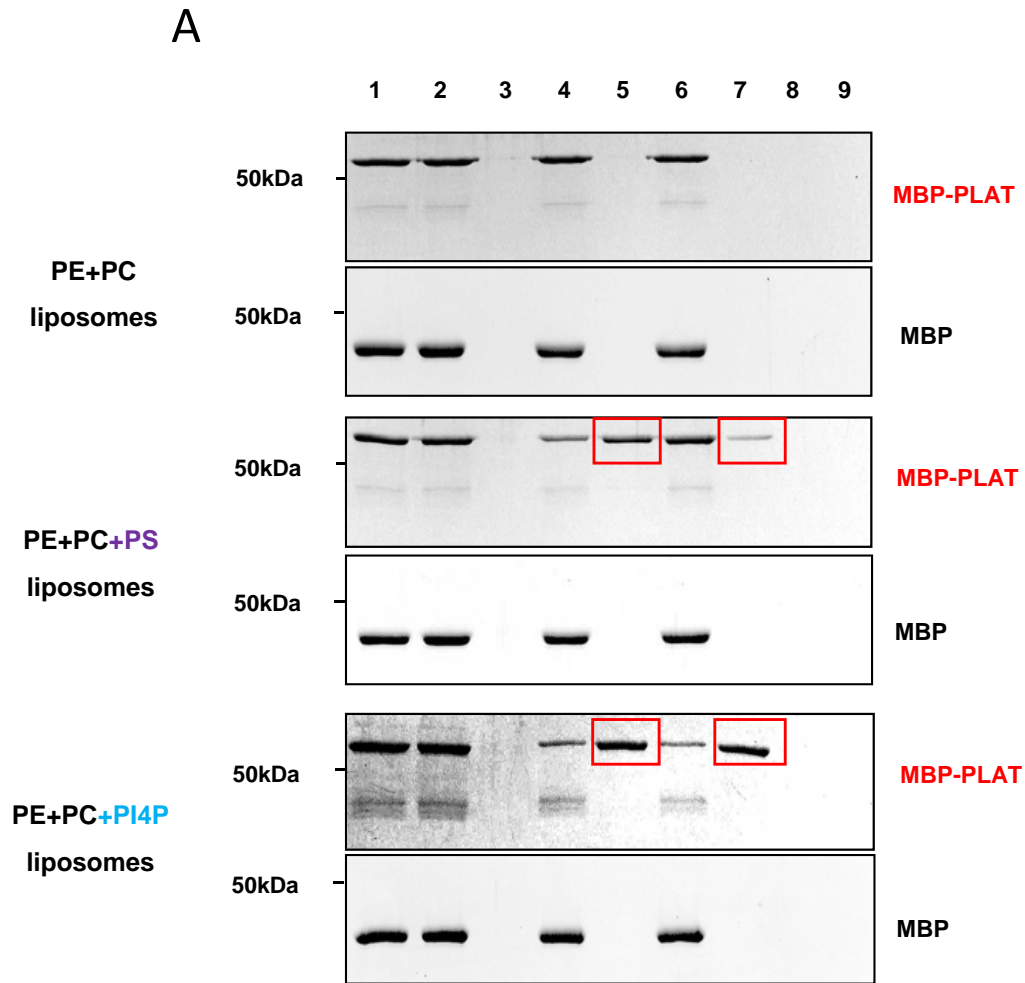
#### Supplementary Figure 12. *Pkd1* Knockdown in *Xenopus* Embryos

A. Verification of the efficacy of the *Pkd1-sMO* by RT-PCR using embryos injected with different concentrations of the MO and analyzed at stages 35 and 40. The asterisks indicate the unspliced products. Note that upon injection of the *Pkd1-sMO*, the main band shifts lower.

B. Schematic diagram showing the spliced mRNAs in the presence or absence of the *Pkd1-sMO*. The lower bands of the PCR were cloned and ten clones were sequenced. The three different identified PCR products are depicted on the right. Note that the *Pkd1-sMO* caused one of two mis-splicing events, each resulting in a truncated protein.

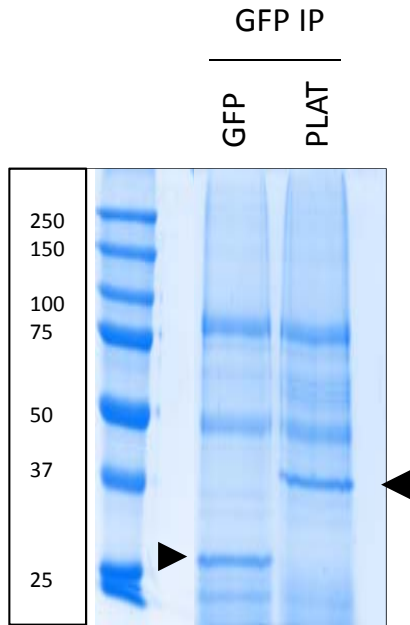
(C-G') Whole mount *in situ* hybridization of uninjected control and *Pkd1-sMO*-injected embryos at stage 39 with *Nbc1* (C,C'), *Sglt1K* (D,D'), *Nkcc2* (E,E'), *Ncc* (F,F') and b1-*Na/K-ATPase* (G,G'). Arrows indicate the expression of *Nbc1* in the DT1 distal tubular segment. Note that in accordance with the criteria for the PKD phenotype in *Xenopus*, none of these markers are lost or grossly altered apart from *Nbc1*.





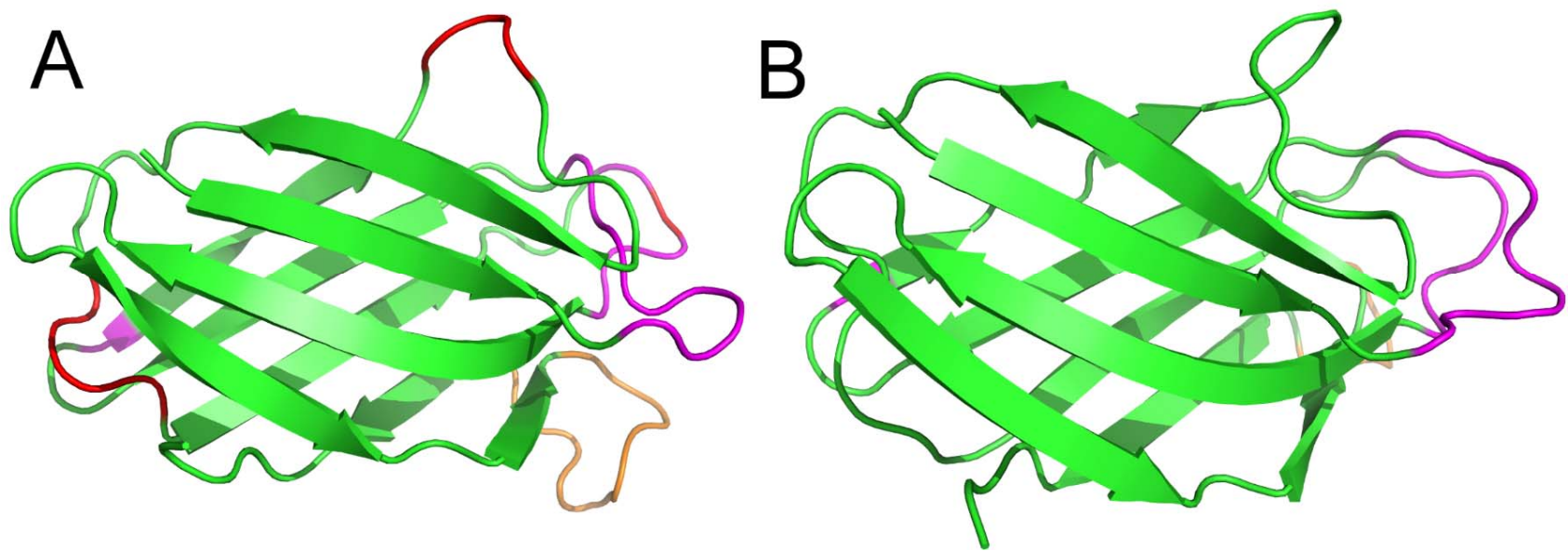


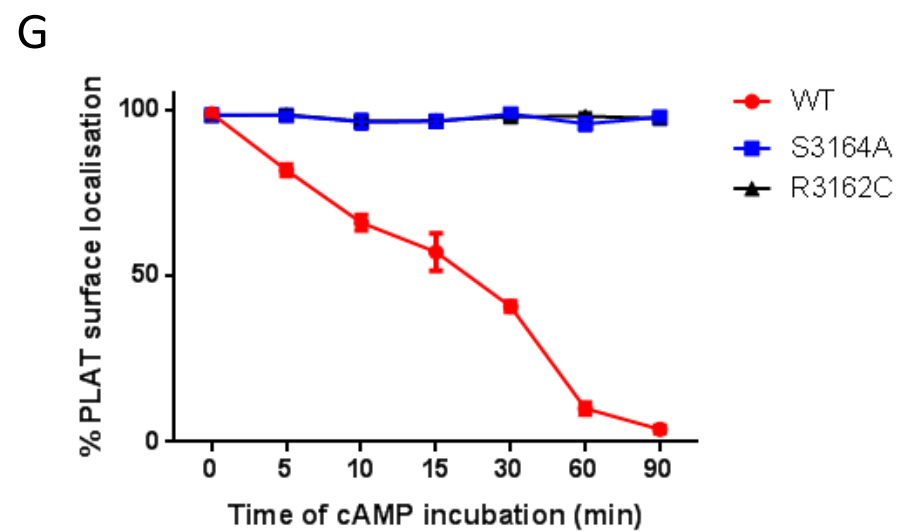
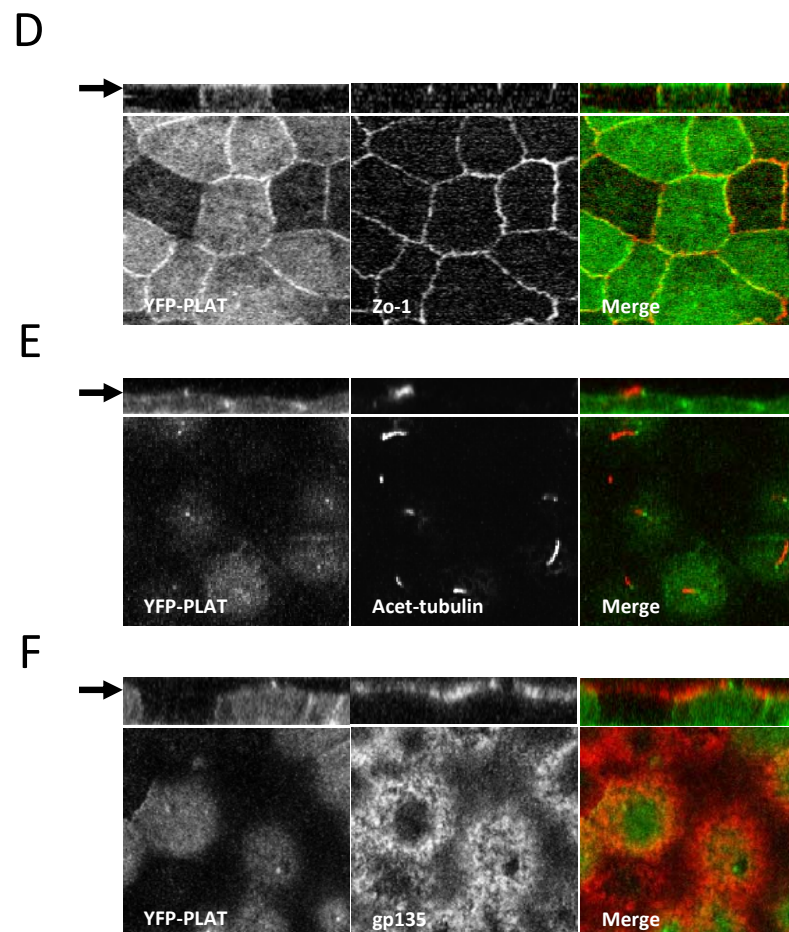
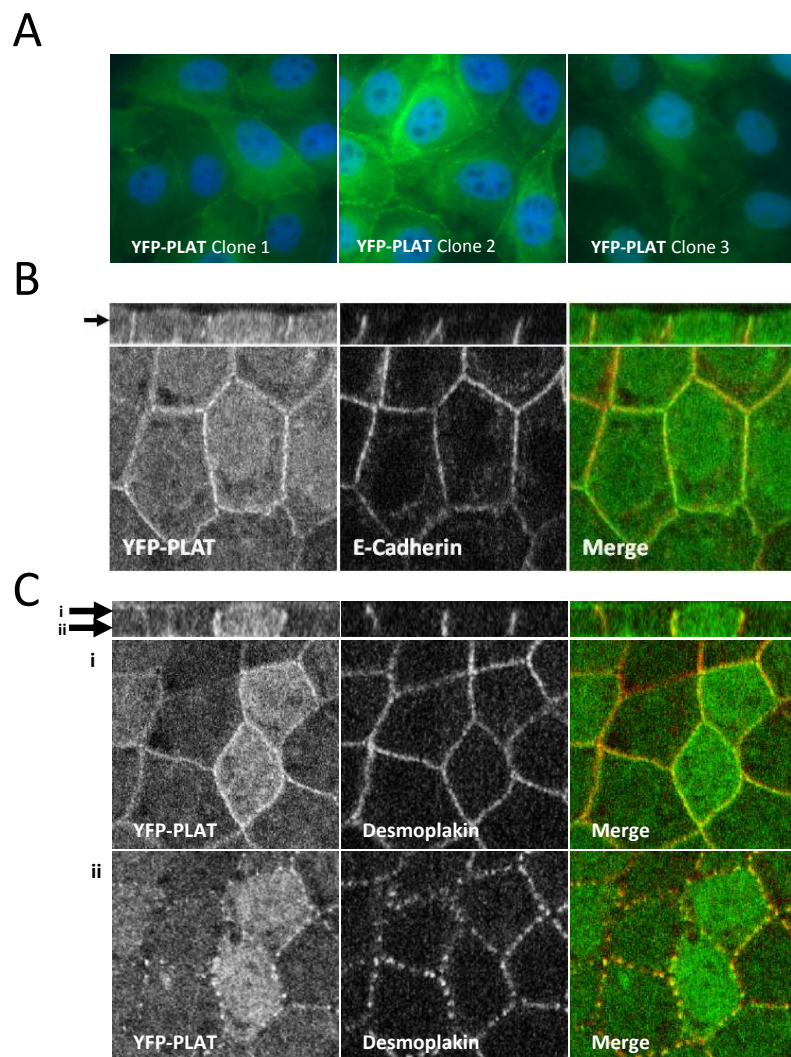
A



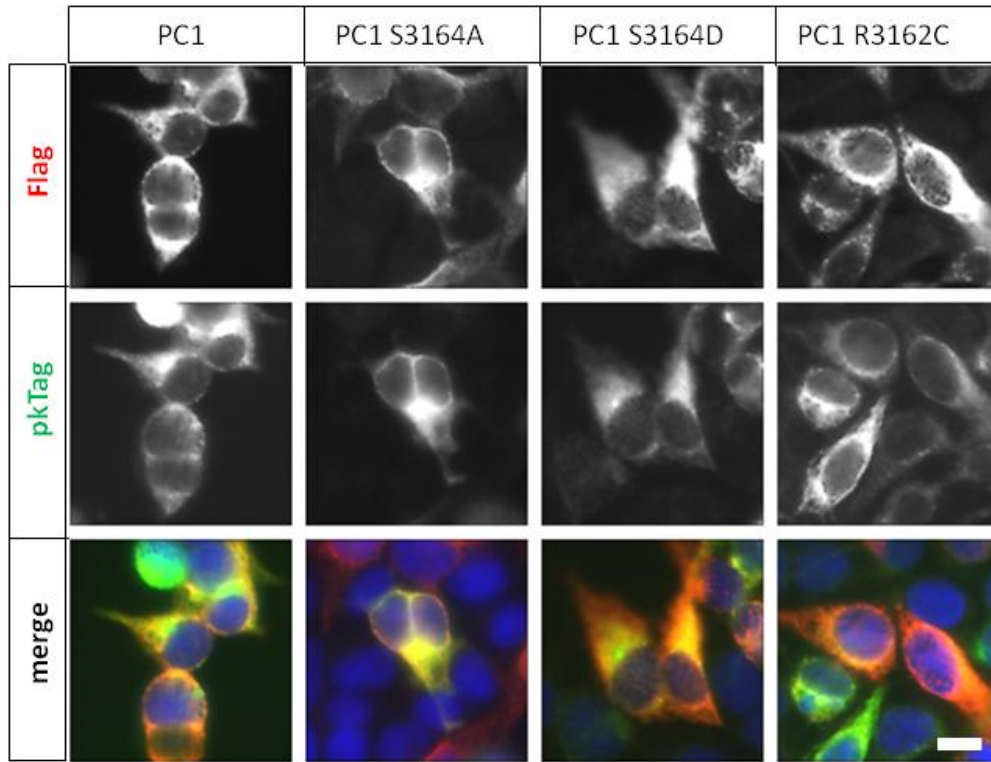
B

Protein Identified	Number of unique peptides	% coverage	Phosphorylation site
Polycystin-1 (PLAT)	7 IATPHSLGSVWK GSGTTAHVGIMLYGVDSR YEILVK GLSPAFLQHVIVR NpSLDIFR GSGTTAHVGIMLYGVDSR SAFFLVNDWLSVETEANGGLVEK	69.82	NpSLDIFR (S3164)
AP2A1	12 IAGDYVSEEVWYR LVEcLETVLNK LLGFGSALLDNVDPNPENFVGAGIIQTK GLAVFISDIR LEPNAQAQMYR DFLTPLLSVR FINLFPETK ALLLSTYIK IVSSASTDLQDYTYFVPAPWLSVK ILVAGDSMDSVK VGGYILGEFGNLIAGDPR AcNQLGQFLQHR	17.3	
AP2A2	19 IAGDYVSEEVWYR YGGTFQNVSVK LTEcLETILNK EMAEAFAGEIPK LSTVASTDILATVLEEMPPPER ILVAGDTMDSVK TSVSLAVSR GLAVFISDIR FVNLFPVK VIQIVINR TTQIGcLLR IVTSASTDLQDYTYFVPAPWLSVK AVDLLYAMcDR ALLLSTYIK LSTVASTDILATVLEEmPPPER VGGYILGEFGNLIAGDPR THIETVINALK AcNQLGQFLQHR VVHLLNDQHLGVVTAATSLITLAQK	25.48	
AP2B1	18 VNYVVQEAVVIR APEVSQYIYQVYDSILK LTNGIWILAELR LAPPLVTLLSGEPEVQYVALR DIPNENELQFQIK LVYLYLMNYAK EYATEVDVDFVR LHDINAQMVEDQGFLDSLRL AAMIWIVGEYAER NVEGQDMLYQSLK LLSTDPVTAK NINLIVQK KGEIFELK NVEGQDmLYQSLK AVWLPAVK KPSETQELVQQVLSLATQSDSNPDLR FLELLPK DcEDPNLIR	23.59	
AP2M1	8 IPTPLNTSGVQVlcmK EEQSQITSQVTGQIGWR ASENAIVWK ESQISAEIELLPTNDK IPTPLNTSGVQVlcmK mIGGLFIYNHK DIILPFR SYLSGmPeCK	19.77	

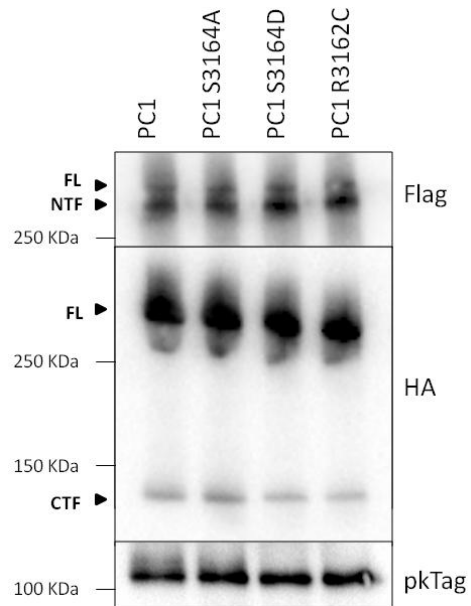




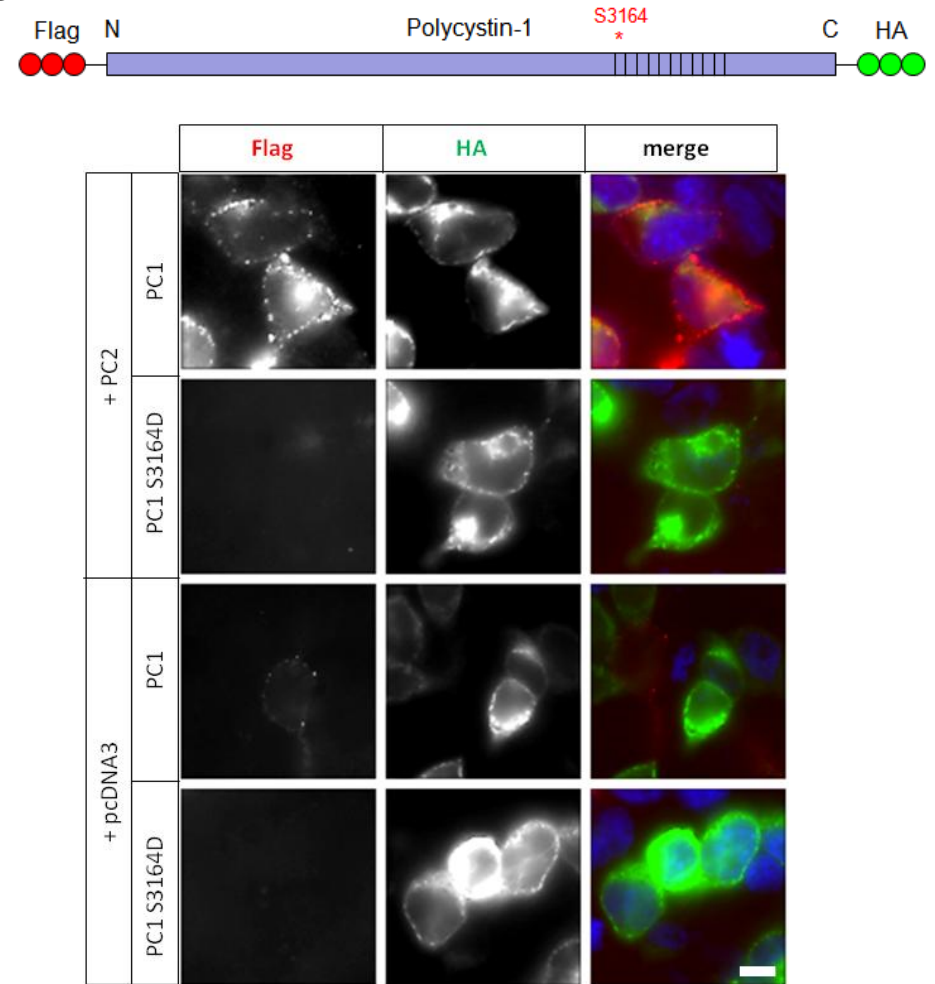
A



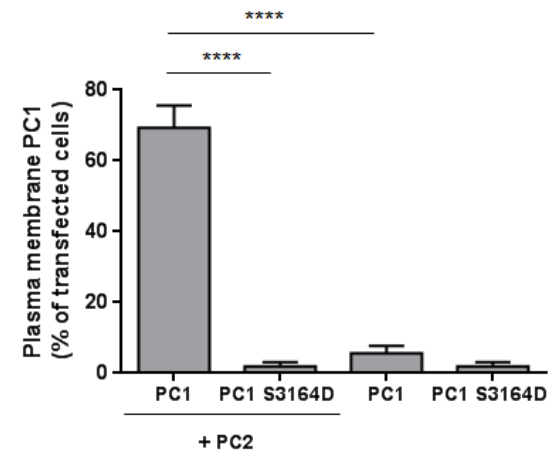
B

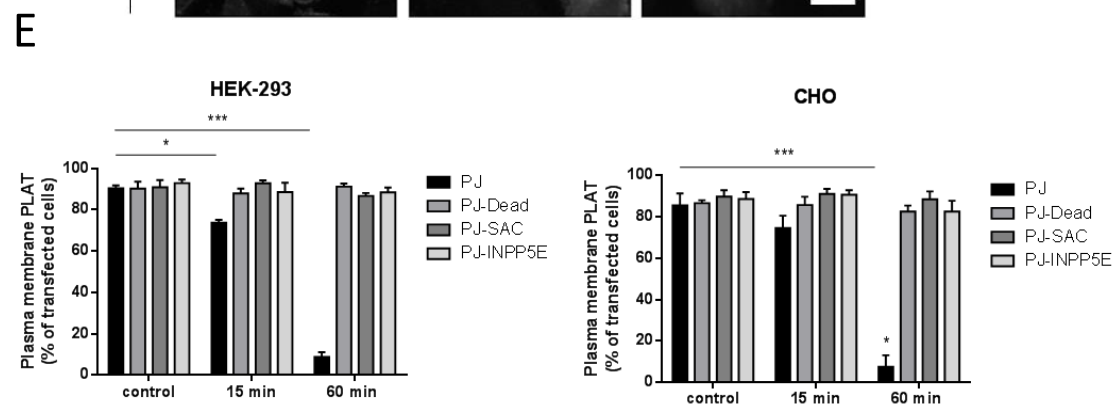
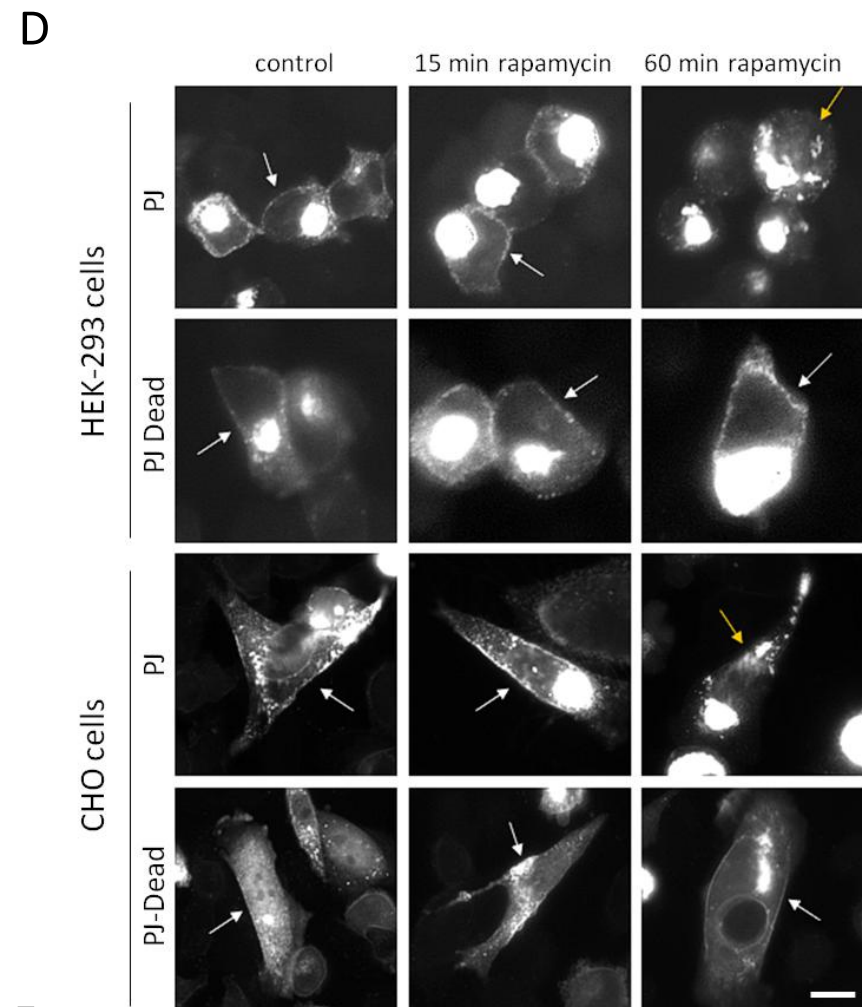
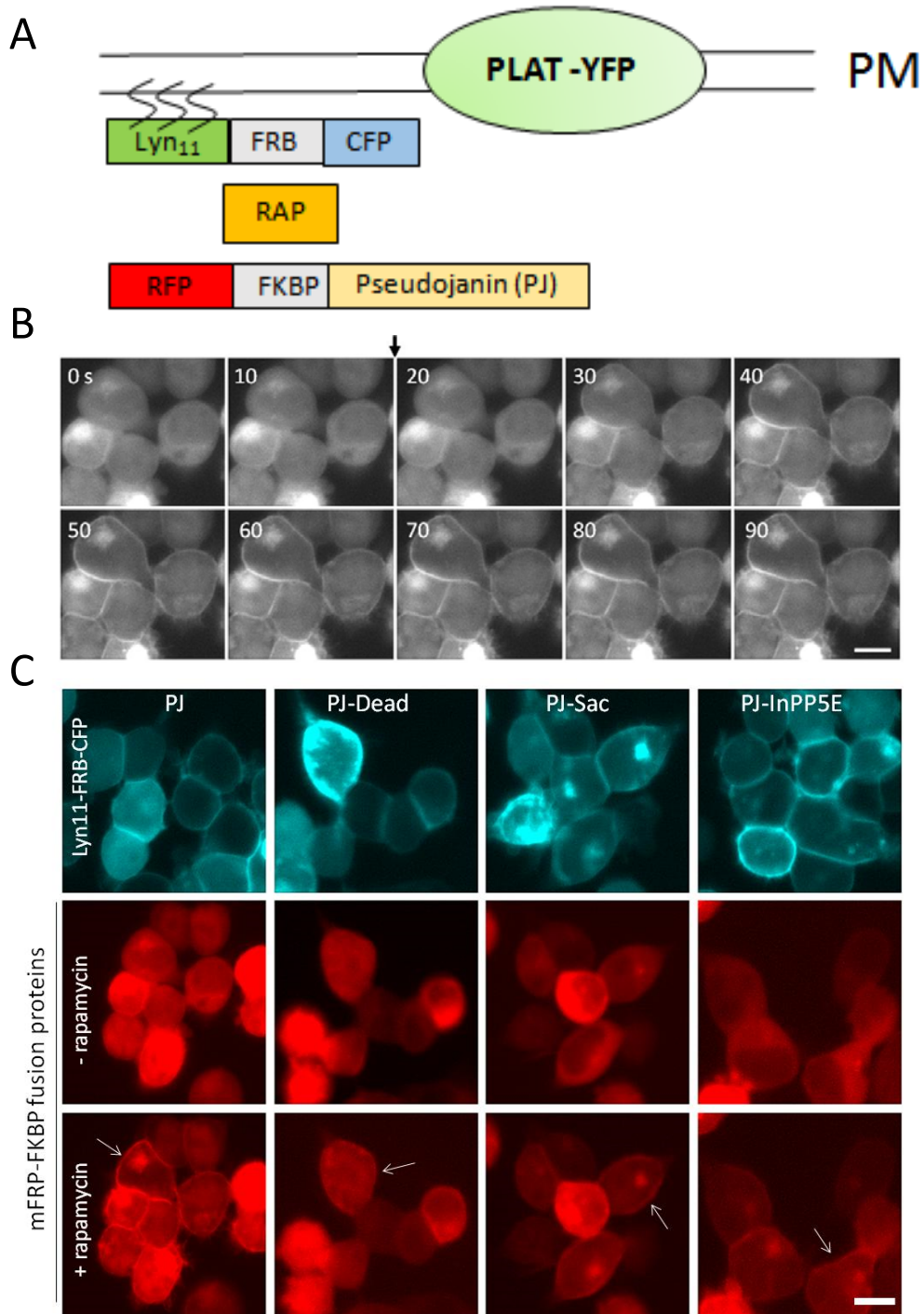


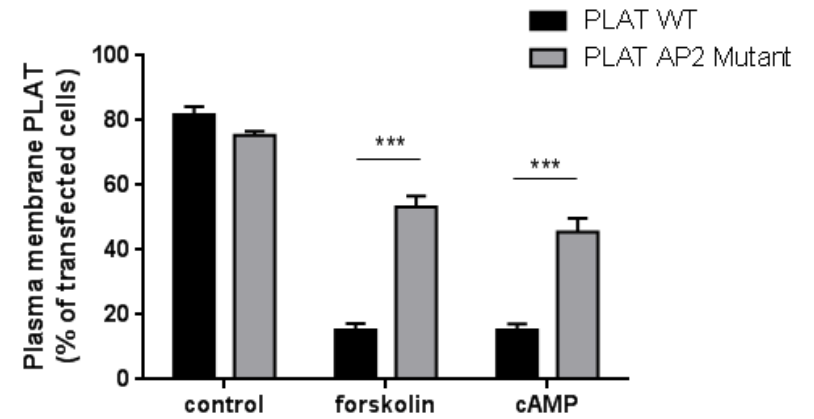
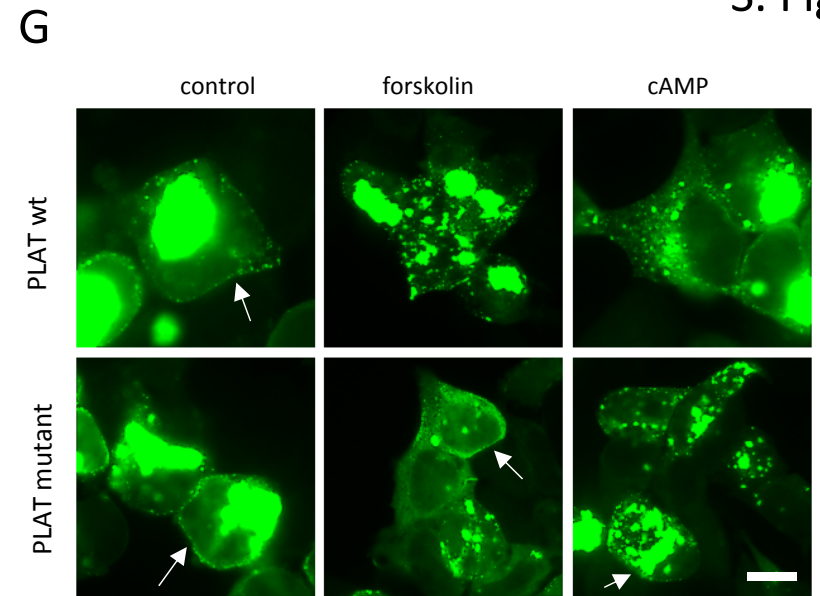
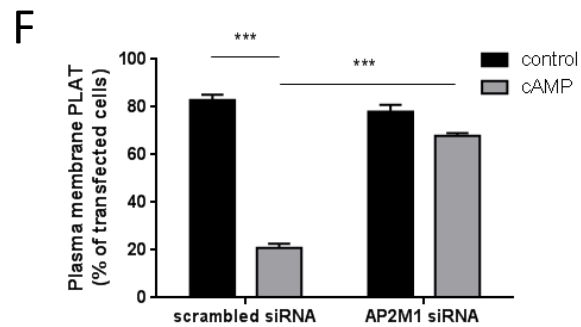
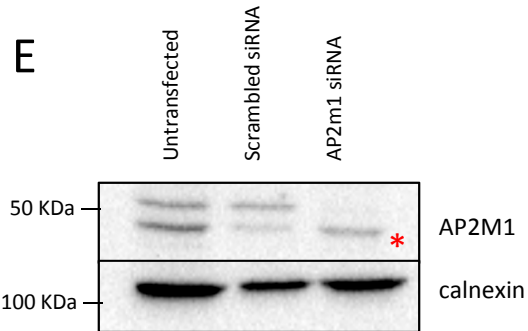
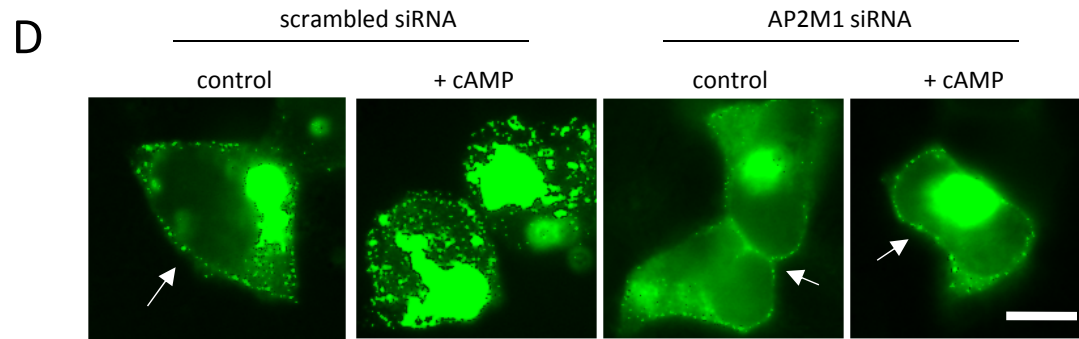
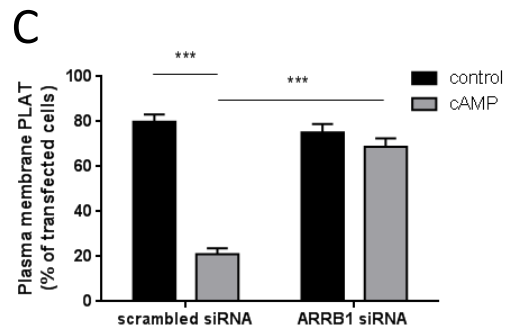
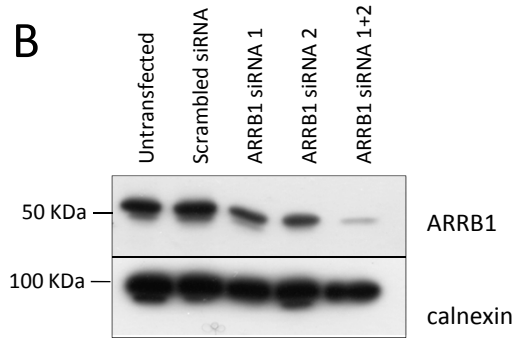
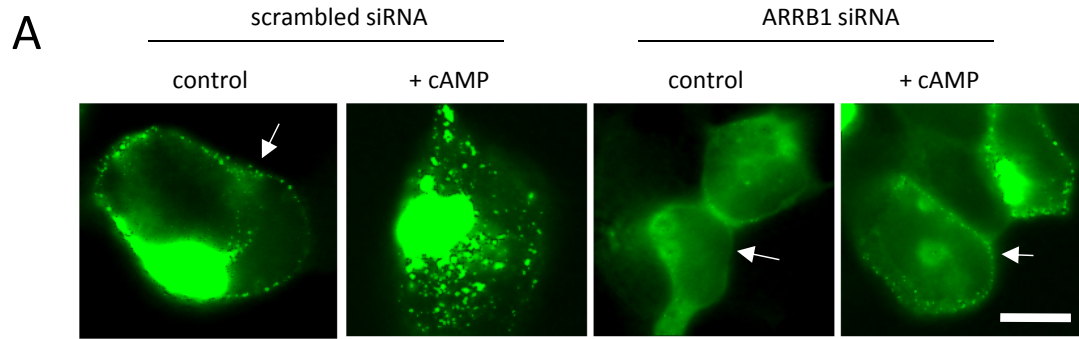
C

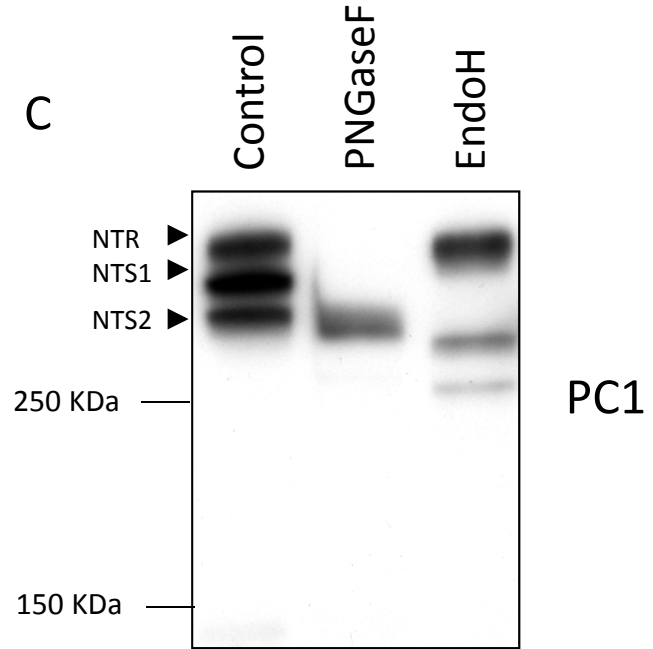
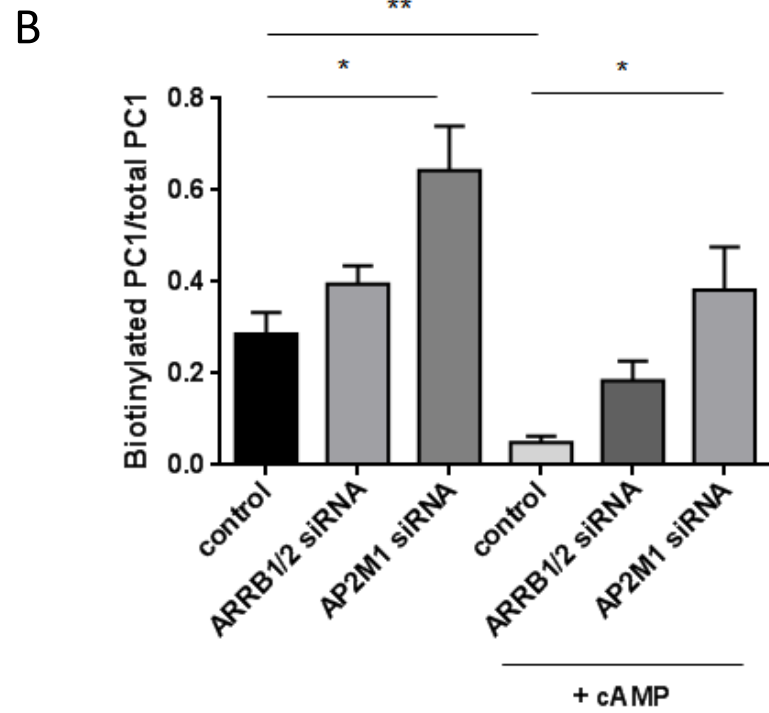
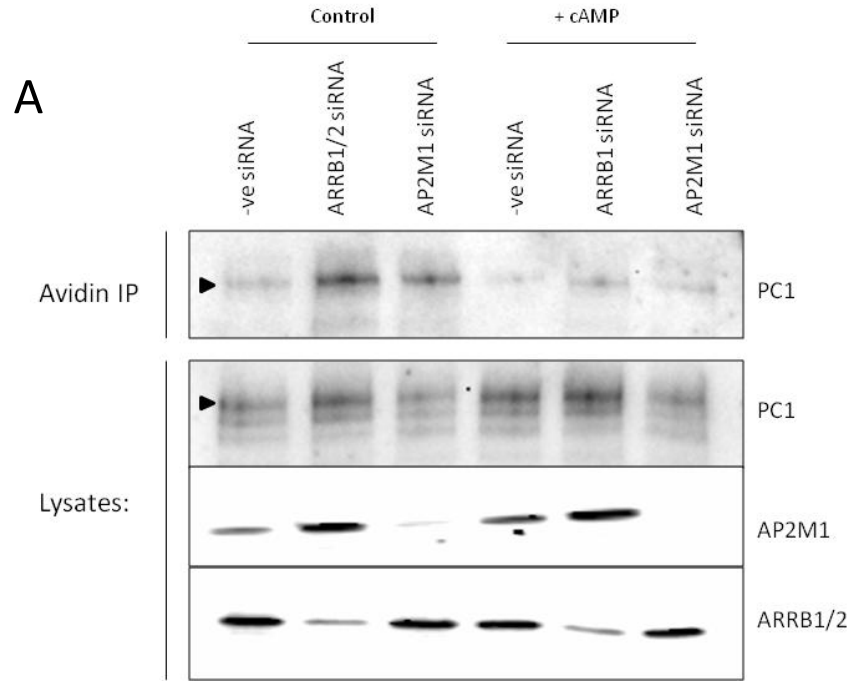


D

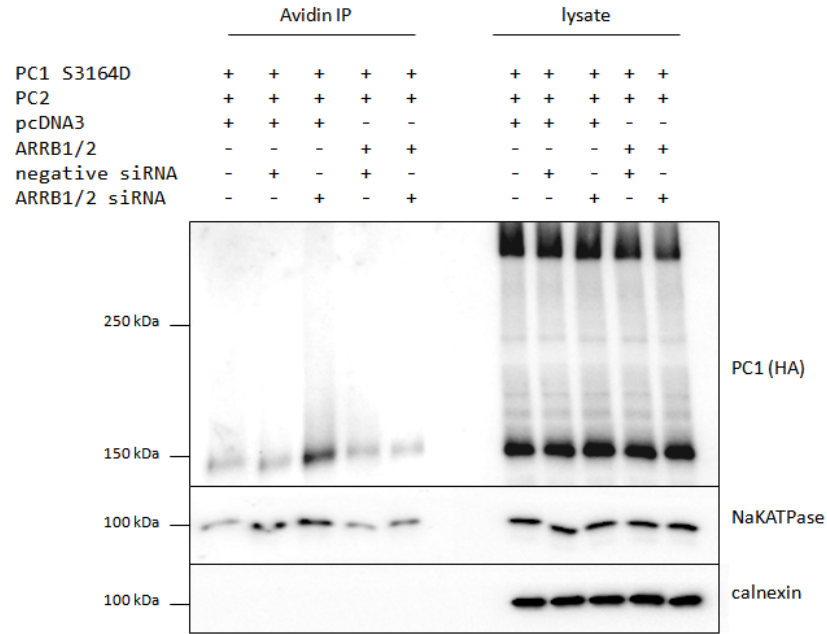




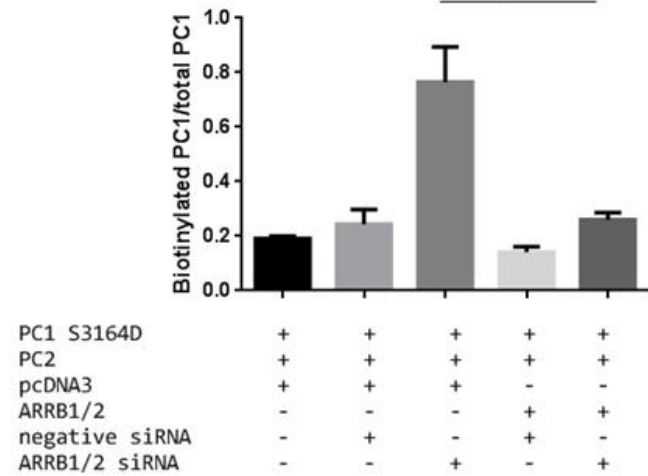




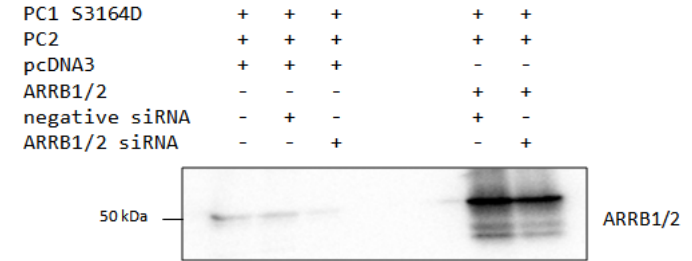
A



B



C



D

